

Optimization of micropatterned poly(lactic-co-glycolic acid) films for enhancing dorsal root ganglion cell orientation and extension

Ching-Wen Li¹, Brett Davis², Jill Shea², Himanshu Sant³, Bruce Kent Gale³, Jayant Agarwal^{2,*}

¹ Department of Mechanical Engineering, National Chung Hsing University, Taichung, Taiwan, China

² Department of Surgery, School of Medicine, University of Utah, Salt Lake City, UT, USA

³ Department of Mechanical Engineering, University of Utah, Salt Lake City, UT, USA

Abstract

Nerve conduits have been a viable alternative to the 'gold standard' autograft for treating small peripheral nerve gap injuries. However, they often produce inadequate functional recovery outcomes and are ineffective in large gap injuries. Ridge/groove surface micropatterning has been shown to promote neural cell orientation and guide growth. However, optimization of the ratio of ridge/groove parameters to promote orientation and extension for dorsal root ganglion (DRG) cells on poly(lactic-co-glycolic acid) (PLGA) films has not been previously conducted. Photolithography and micro-molding were used to define various combinations of ridge/groove dimensions on PLGA films. The DRG cells obtained from chicken embryos were cultured on micropatterned PLGA films for cell orientation and migration evaluation. Biodegradation of the films occurred during the test period, however, this did not cause deformation or distortion of the micropatterns. Results from the DRG cell orientation test suggest that when the ridge/groove ratio equals 1 (ridge/groove width parameters are equal, *i.e.*, 10 μm /10 μm (even)), the degree of alignment depends on the size of the ridges and grooves, when the ratio is smaller than 1 (groove controlled) the alignment increases as the ridge size decreases, and when the ratio is larger than 1 (ridge controlled), the alignment is reduced as the width of the grooves decreases. The migration rate and neurite extension of DRG neurons were greatest on 10 μm /10 μm and 30 μm /30 μm micropatterned PLGA films. Based on the data, the 10 μm /10 μm and 30 μm /30 μm micropatterned PLGA films are the optimized ridge/groove surface patterns for the construction of nerve repair devices.

*Correspondence to:

Jayant Agarwal, M.D.,
jay.agarwal@hsc.utah.edu.

orcid:

0000-0002-1209-6703
(Jayant Agarwal)

doi: 10.4103/1673-5374.224377

Accepted: 2017-11-14

Key Words: nerve regeneration; nerve repair; neural cell migration; neural cell alignment; micropattern; dorsal root ganglion; topological cues; neural regeneration

Introduction

Peripheral nerve injuries commonly lead to permanent loss of motor and sensory function if complete nerve regeneration does not occur (Navarro et al., 2007). Nerve injuries can have varying degrees of severity with the most severe being characterized by complete transection of all the axons and connective tissue. Nerve gaps greater than 2 cm are typically treated with an autologous nerve graft, decellularized allografts, or bioresorbable nerve conduits. Autografts are the current 'gold standard' for large gap injury repair. Use of autograft leads to the loss of function at the donor nerve site and therefore has limited donor sources. In addition, functional recovery after autograft repair is frequently inadequate (Battiston et al., 2005).

Developing and translating medical technologies that can match or improve patient outcomes to the autograft has become one of the most commonly attempted problems to be solved in the field of peripheral nerve regeneration. Nerve conduits made of various biomaterials, enhanced by topological cues, nerve growth factors, other small molecules, inner lumen scaffolding, and nerve/stem cell seeding have been studied (Daly et al., 2013; Arslantunali et al., 2014; Reichenberger et al., 2016). Additionally, allografts, decellularized allografts, and xenografts have been investigated in an attempt to replace the autografts. Superior nerve conduits are not only expected to grossly connect both ends of the

severed nerve, but also are expected to promote and guide axonal growth. Hence, an ideal nerve conduit design must incorporate a way to mimic the native physical environment, release neurotrophic factors, and be able to promote neurite elongation. Surface topology is one method to affect cell behavior by mimicking the native extracellular matrix (ECM) environment. Many studies have tried to control neural cell behaviors (migration, alignment, proliferation) through engineered micro- or nano-environmental scaffolding for use in peripheral nerve reconstruction. Previous studies have demonstrated that nerve cells grow along longitudinally aligned scaffolding consisting of micro-grooved structure and micro-topological cues which could provide long term stimulation for cell proliferation. Yang et al. (2005) fabricated an aligned poly-L-lactic acid (PLLA) nano/micro fibrous scaffolds for neural regeneration by electrospinning. They have demonstrated that the rate of neural stem cell differentiation was higher for PLLA nanofibers than that of micro fibers and it was independent of the fiber alignment. At the same time, poly(lactic-co-glycolic acid) (PLGA) nanofiber conduits were examined using a rat sciatic nerve model with a 10 mm long gap and successful nerve regeneration was demonstrated (Bini et al., 2004; Sudwilai et al., 2014).

Micropatterned surfaces have been shown to improve nerve cell alignment and accelerate growth longitudinally (Mobasserri et al., 2013; Li et al., 2014). However, there is less

discussion on optimal combinations of ridge/groove micropatterns for aligned cells and migration abilities. In this study, we investigated the *in vitro* nerve cell growth optimization to determine the optimal ridge/groove ratio to accelerate neurite extension and cell alignment. A photolithographic technique was developed to fabricate various ridge/groove ratio micropatterned PLGA films. Dorsal root ganglion (DRG) cells were cultured on various micropatterned PLGA films to investigate the cell alignment and migration ability.

Materials and Methods

PLGA solution preparation

75/25 PLGA pellets purchased from Evonik Co (Essen, Germany) were used to manufacture the films. 10 g of PLGA particles were dissolved in 20 mL of acetone and stirred at 60 r/min at room temperature for 2 hours. 6 mL of 100% ethanol was added and stirring continued at room temperature overnight.

Fabrication of micropatterned PLGA films

A diagram showing PLGA micropatterned film fabrication process is shown in **Figure 1**. **Figure 1** presents the various ridge/groove films fabricated and tested.

A photolithography process was performed to produce various combinations of ridge/groove micropattern molds on a silicon substrate (**Figure 1A**). The silicon substrate was cleaned and AZnLOF2020 negative photoresist was coated on the surface by spin coating with a series of rotating speeds (30 r/min 5 seconds, 500 r/min 5 seconds and 1,400 r/min 45 seconds). The silicon substrates were soft baked at 110°C using a hotplate for 1 minute. Silicon substrates with photoresist were exposed to UV light by a mask aligner (Hybralign Series 200, OAI, San Jose, California, USA) for 8.5 seconds. AZ 1:1 developer solution was used for development for 45 seconds, and then rinsed in DI water for 1 minute. Substrates were dried by N₂ gas, and the silicon substrate photoresist mold was obtained. 50 µL of saline was used as a mold releasing agent, saline was evaporated from the silicon photoresist surface in a vacuum chamber for 1 hour. 20 mL of polydimethylsiloxane (PDMS) (1:10) solution was added to the photoresist mold and degassed in a vacuum chamber for 1 hour and baked in an oven at 65°C overnight for crosslinking (**Figure 1B**). The final PDMS mold was removed from the photoresist mold and 7 mL of the PLGA solution was poured onto the mold. It was put into a 10 cm² glass dish and surrounded by 5 mL acetone on a 35°C hotplate for 1 hour to degas (**Figure 1C**). After drying at room temperature overnight, the PLGA film was demolded from the PDMS mold to obtain a micropatterned PLGA film (**Figure 1D**).

Material degradation rate estimation

Before the degradation test was initiated, the micropatterned PLGA films were dried and weighed (W_0). The PLGA films were sterilized by ethylene oxide and placed into a 24-well culture plate, 1 film/well. 1 mL of DRG culture medium was added to each well, and the 24-well culture plates were kept in a cell culture incubator under 5% CO₂ and 37°C conditions for 14 days. The PLGA films were collected after the

first 7 days and washed with PBS three times. After drying at 30°C for 2 days, the weight was measured again (W_1). The PLGA films were then re-sterilized in 24-well culture plates and the incubation process was repeated. Five samples were used in this test. The PLGA film drying and weighing process was repeated to obtain the day 14 weights (W_2). The material degradation rate was calculated as equation (1).

$$\text{Material degradation rate (\%)} = \frac{W_0 - W_n}{W_0} \times 100\% \quad (1)$$

W_0 represents the material dry weight before degradation; W_n was material dry weight after degradation, $n = 1$ or 2 represents the degradation time (days).

DRG cell dissection, disassociation, and culture

To distinguish the effects that different ridge/groove combinations have on peripheral nerve cells, we prepared primary cell cultures containing a mixture of neuronal and glial cells from harvested DRGs of E10 chicken embryos (Merrill's Egg Farm, Emmett, ID, USA). The use of chicken embryos did not require IACUC approval. Tissue types were carefully dissected and dissociated with 0.25% trypsin for 10 minutes at 37°C. The disassociated DRG cell mixture was suspended in Dulbecco's modified Eagle medium (DMEM) supplemented with 10% fetal bovine serum, 5 ng/mL nerve growth factor, and 1% Gibco™ antibiotic-antimycotic (penicillin, streptomycin, fungizone™). Suspension was centrifuged at 1,000 r/min for 10 minutes, cell concentration was adjusted to 1×10^5 cells/mL to seed on 75 cm² tissue culture flasks and incubated at 37°C and 5% CO₂. The culture medium was changed 24 hours later. When cell confluency was approximately 80–90%, the cells were passaged. Passages 4–6 cells were used in this study.

Disassociated nerve cells cultured on micropatterned PLGA films

Micropatterned PLGA films were sterilized by ethylene oxide, and then put into a 10 cm² culture dish. Cells were trypsinized and cell concentration was adjusted to 2×10^4 cells/300 µL for culturing on PLGA films overnight. 10 mL of culture medium described earlier was added to the culture dish and incubated for 3 days at 37°C and 5% CO₂. Each group contained two samples ($n = 2$). Flat PLGA films were used as a control group.

Whole DRGs cultured on micropatterned PLGA films for neurite extension distance measurement

In order to estimate the DRG neurite extension rate and distance, whole DRGs collected from chicken embryos were cultured with 200 µL of DMEM supplemented with 10% fetal bovine serum, 5 ng/mL nerve growth factor and 1% Gibco™ antibiotic-antimycotic (penicillin, streptomycin, fungizone™), plated at the edge of a micropatterned PLGA film and incubated at 5% CO₂ and 37°C overnight. After 10 mL of the culture medium was added to the culture dish, the whole DRGs were cultured for 3 days at 5% CO₂ and 37°C on 10 µm/10 µm, 30 µm/30 µm, and 100 µm/30 µm micropatterned and flat PLGA films for assessing neurite

extension. One film from each group was used. The average neurite length (l_{avg}) was calculated by: $l_{avg} = (A_{tot}/\pi)^{1/2} - (A_{DRG}/\pi)^{1/2}$ (Labroo et al., 2017).

Characterization of cell orientation, migration, and neurite extension by immunofluorescence staining

DRG cells were grown on micropatterned PLGA films, fixed with 2% paraformaldehyde and 0.2% Triton X-100 in PBS for 10 minutes at room temperature, washed three times with PBS, and processed for immunofluorescence staining. After a blocking step with 1% bovine serum albumin for 30 minutes at room temperature, cells were incubated with primary antibody for 1 hour at 37°C. The neuron-specific rabbit anti-beta-tubulin IgG (1:500) was used as the primary antibody. Cells were washed three times in PBS, and then incubated with the second antibody for 1 hour at room temperature in the dark. Secondary antibody goat anti-rabbit IgG Alexa Fluor 568 was diluted in PBS (1:1,000). Cells were incubated with 4',6-diamidino-2-phenylindole (DAPI) diluted in PBS (1:1,000) for nucleus staining. A Nikon Widefield Microscope (Melville, NY, USA) was used for fluorescence microscopy for the recording and analysis of nerve cell growth characteristics on films. Cell orientation was measured for groups: Even (10 μm/10 μm, 30 μm/30 μm, 50 μm/50 μm, 100 μm/100 μm), groove controlled (10 μm/50 μm, 30 μm/50 μm, 10 μm/100 μm, 30 μm/100 μm), ridge controlled (50 μm/10 μm, 50 μm/30 μm, 100 μm/10 μm, 100 μm/30 μm). For each group, three images were selected for measurement of cell orientation. The cell orientation plugin for ImageJ software (NIH, Bethesda, MD, USA) was used to analyze cell positioning on the micropatterned PLGA film (Li et al., 2014).

Characterization of cell morphology by scanning electron microscope (SEM)

Cells grown on micropatterned PLGA films were fixed with 2% paraformaldehyde for 30 minutes. After three PBS washes, cells were dehydrated using a series of ethanol washes (concentrations 70%, 80%, 90%, 95% and 100%) for 30 minutes at each step. The surface was coated with a 5 nm gold film (Thermofisher, Hillsboro, OR, USA) by sputter for conductivity. The FEI Quanta 600 FEG (Thermofisher) at the Utah Nanofab of the University of Utah was used to observe the cell morphologies of the nerve cells grown on the micropatterned PLGA films. ImageJ software was used to quantify cell elongation, and for each group there were three selected images.

Results

Micropatterned PLGA film ridge/groove characterization

During this fabrication process, the dimensions of the ridges and grooves were consistent with the design parameters (Figure 1). These findings suggest that the photolithography and PDMS molding fabrication process was sufficient at producing repeatable films that match the design parameters.

Morphological changes and weight loss of the micropatterned PLGA films

To determine if the micropatterns maintained their original

morphological structure after incubation in culture media at 37°C, the cross-section and surface of films were examined using scanning electron microscopy (Figure 2). The thickness of the micropatterned PLGA film, which was 169.84 μm before the culture medium, was added (Figure 2A). After material degradation for 7 and 14 days, the thickness of the PLGA films increased to 211.05 and 237.27 μm, respectively (Figure 2B and C). The material cross-section was smooth on day 0 (Figure 2A), but wrinkles formed while the material was immersed in the culture media after 7 days (Figure 2B). After 14 days of exposure to the culture media at 37°C, a micro-porous consistency was generated throughout the film (Figure 2C). The micropatterns were still maintained on the surface of the film after exposure to the culture media at 37°C, and swelling of the material did not cause the micropattern structure to deform (Figure 2D and E).

SEM found that morphological changes occurred in the interior and at the surface of the films after prolonged exposure to the incubation environment. During the degradation process, the surface microstructure of the micropatterned PLGA film gradually changed. In the beginning, the micropatterned PLGA film had a transparent appearance and a smooth surface. With time, some small holes were observed on the film surface, and the film became whitish and coarse (Figure 2B and C).

To estimate the material degradation rate, a weight loss study was performed. Data from weight loss study are as follows: Day 0: 63.43 ± 6.90 μg; day 7: 62.1 ± 6.66 μg, and day 14: 60.9 ± 6.45 μg. The data from the weight loss study showed that the material degradation rate was approximately 2% (1 μg) per 7 days and 0.28% (0.14 μg) per day for the first 14 days.

DRG neuron orientation and behavior on micropatterned PLGA films

Figure 3 shows immunofluorescence staining of the DRG neurons on micropatterned PLGA films of various ridge/groove combination ratios. Measurements of the cell orientation on the micropatterned PLGA films are shown in Table 1. The alignment behavior of the DRG neurons was dependent on the ridge/groove combination. Cells became longer in morphology when the DRG neurons were cultured on the micropatterned PLGA films of even ridge/groove ratio (Figure 3; left column). Also the cells presented alignment behavior and the cells had less axonal branching when grown on the micropatterned PLGA films, especially on the 10 μm/10 μm combination. In contrast, the cells cultured on the films with either ridge or groove parameter set at 100 μm wide were longer and less branched than when cultured on flat films (Figure 3; 10 μm/100 μm, 30 μm/100 μm, 100 μm/10 μm and 100 μm/30 μm).

In Table 1, in the groups with even ridge/groove ratios increased, the angle of the cell relative to the micropattern increased. When cells were cultured on micropatterned PLGA films with non-even ridge/groove ratios, the cell orientations displayed inverse results (Table 1). In the groove control group, the angle of the cells relative to the micropattern increased with the increase of the ridge width. The cells pos-

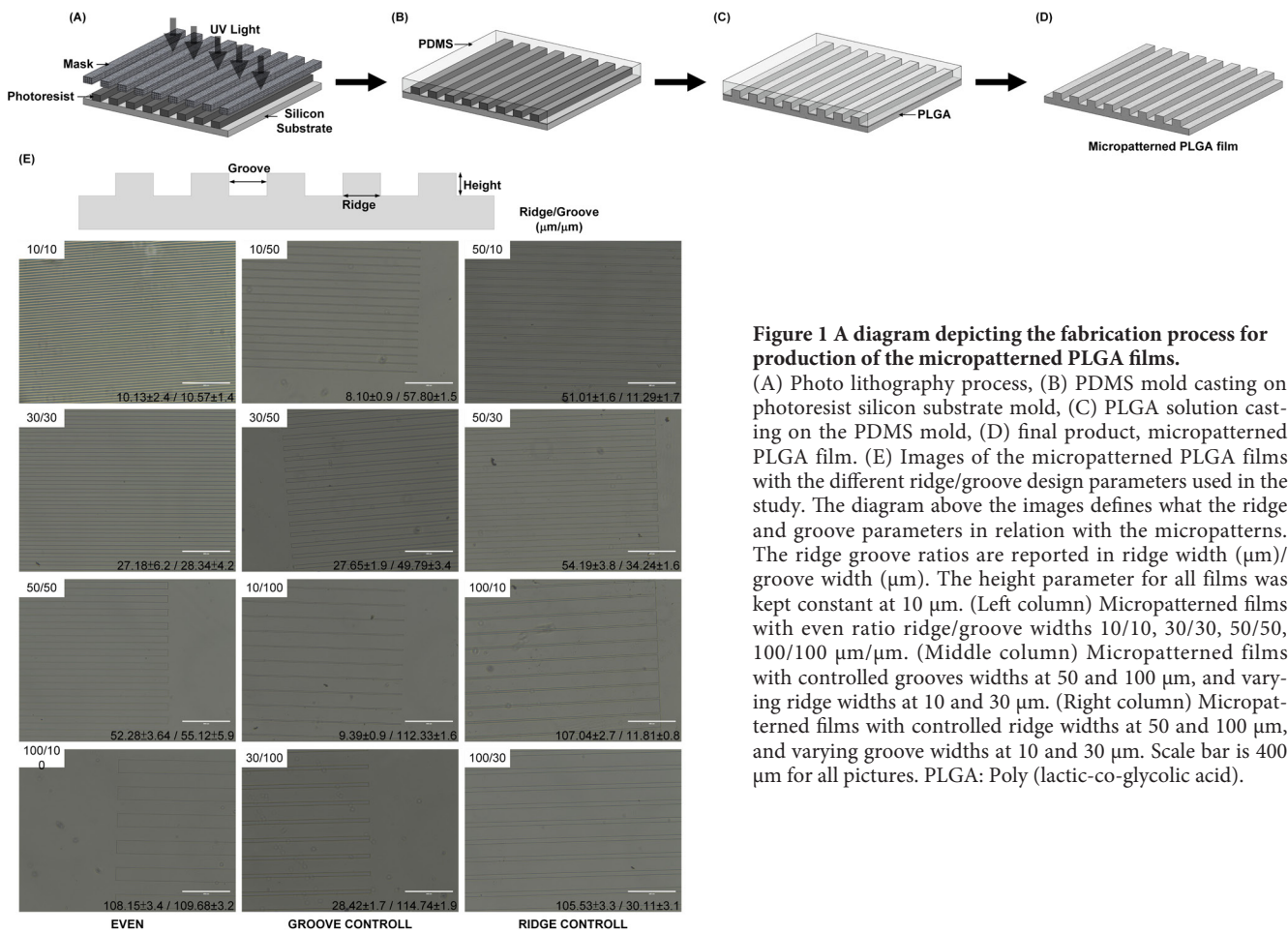


Figure 1 A diagram depicting the fabrication process for production of the micropatterned PLGA films.

(A) Photo lithography process, (B) PDMS mold casting on photoresist silicon substrate mold, (C) PLGA solution casting on the PDMS mold, (D) final product, micropatterned PLGA film. (E) Images of the micropatterned PLGA films with the different ridge/groove design parameters used in the study. The diagram above the images defines what the ridge and groove parameters in relation with the micropatterns. The ridge groove ratios are reported in ridge width (μm)/groove width (μm). The height parameter for all films was kept constant at $10\ \mu\text{m}$. (Left column) Micropatterned films with even ratio ridge/groove widths $10/10$, $30/30$, $50/50$, $100/100\ \mu\text{m}/\mu\text{m}$. (Middle column) Micropatterned films with controlled grooves widths at 50 and $100\ \mu\text{m}$, and varying ridge widths at 10 and $30\ \mu\text{m}$. (Right column) Micropatterned films with controlled ridge widths at 50 and $100\ \mu\text{m}$, and varying groove widths at 10 and $30\ \mu\text{m}$. Scale bar is $400\ \mu\text{m}$ for all pictures. PLGA: Poly (lactic-co-glycolic acid).

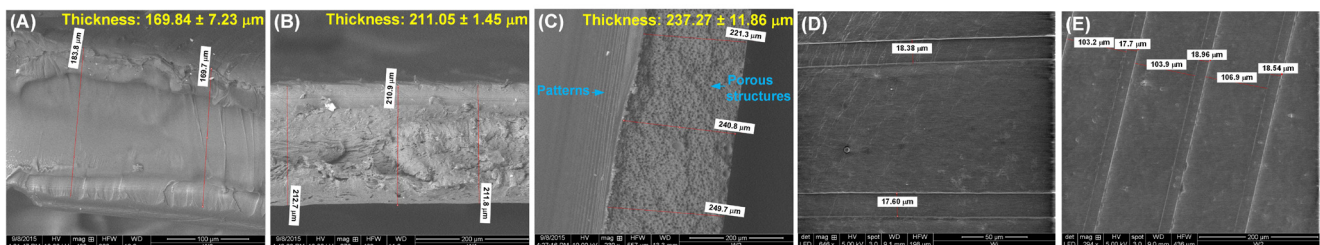


Figure 2 Scanning electron microscope images of the cross-sections and surface of the micropatterned PLGA film.

Scanning electron microscope images of the cross-sections of the micropatterned PLGA film before and after material degradation at 0 (A), 7 (B), and 14 days (C). (D) and (E) are images of the surface of the micropatterned PLGA films at 7 and 14 days, respectively ($n = 3$). Scale bars: $100\ \mu\text{m}$ in A, $200\ \mu\text{m}$ in B, C, and E, $50\ \mu\text{m}$ in D. PLGA: Poly(lactic-co-glycolic acid).

Table 1 Dorsal root ganglion cell orientation angle in relation to the ridge lines when grown on the micropatterned poly(lactic-co-glycolic acid) films of various ridge/groove combination ratios

Even (degree)	Groove controlled (degree)	Ridge controlled (degree)
1.51 ± 0.76 (10/10)	4.14 ± 1.63 (10/50)	63.53 ± 21.05 (50/10)
4.39 ± 2.57 (30/30)	24.23 ± 9.29 (30/50)	4.81 ± 2.78 (50/30)
9.28 ± 8.72 (50/50)	6.77 ± 3.07 (10/100)	92.99 ± 22.13 (100/10)
13.1 ± 5.75 (100/100)	65.14 ± 27.45 (30/100)	2.83 ± 1.89 (100/30)

Ridge/groove parameter ($\mu\text{m}/\mu\text{m}$) combination indicated in parenthesis next to data point.

essed good orientation at $10\ \mu\text{m}$ ridge widths. In the groove controlled group, the width of groove was relatively large compared to the ridge width and cell size, therefore ridge patterns were recognized as micro-wires for cell guidance.

Figure 4A and **B** shows the DRG cells cultured on the $10\ \mu\text{m}/10\ \mu\text{m}$, $100\ \mu\text{m}/100\ \mu\text{m}$, $10\ \mu\text{m}/50\ \mu\text{m}$, and $50\ \mu\text{m}/10\ \mu\text{m}$ micropatterned PLGA films. Cells crossed over the grooves to connect to both edges of the ridges. But the dimensions of the grooves on the $100\ \mu\text{m}/100\ \mu\text{m}$ PLGA films were larger than a single cell's size, therefore there was less physical cues to provide cell guidance. In contrast, the $10\ \mu\text{m}/10\ \mu\text{m}$ combination showed a strong ability to guide cell growth and alignment. In the inconsistent combination groups ($10\ \mu\text{m}/50\ \mu\text{m}$ and

50 $\mu\text{m}/10 \mu\text{m}$), cells were aligned with the edge of ridges on the 10 $\mu\text{m}/50 \mu\text{m}$ combination films (Figure 4C), and cells on the 50 $\mu\text{m}/10 \mu\text{m}$ combination films presented inverse responses where most of the cell bodies were located on the ridges and crossed over the grooves (Figure 4D).

DRG cell neurite extension behavior on micropatterned PLGA films

Since the DRG neurons showed good alignment properties

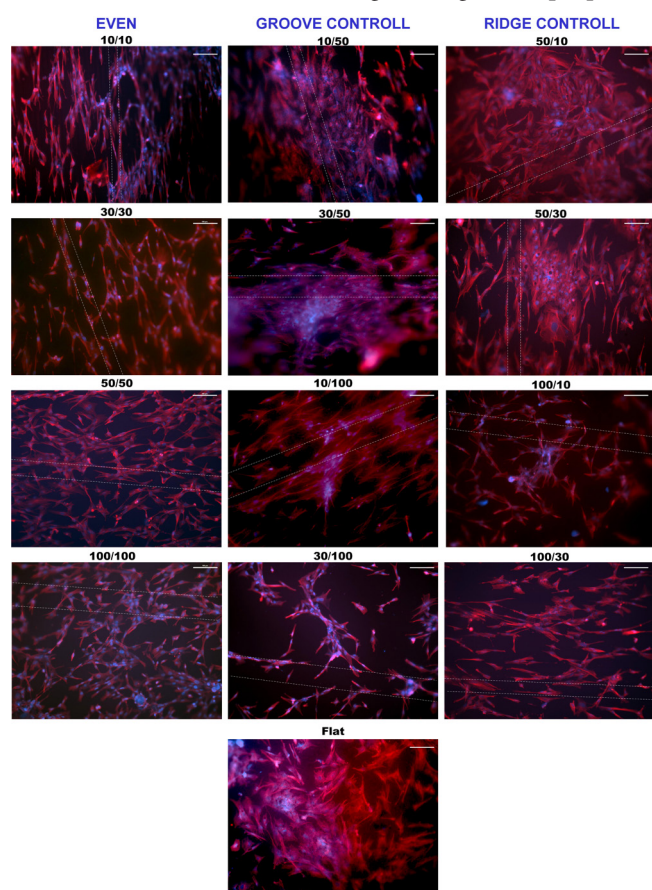


Figure 3 Immunolabeled DRG neurons on various ridge/groove combination micropatterned PLGA films.

The red fluorescence labels beta-tubulin protein which is a neuronal marker. Blue DAPI stain indicates labeled nuclei. Scale bars: 100 μm . The white dotted line represents the micropattern orientation. DRG neuron cell alignment decreased as the ridge and groove width increased in the even ratio group (left column). When groove parameter was controlled, DRG neuron cell alignment decreased as the ridge width was increased (middle column). When ridge parameter was controlled, DRG neuron cell alignment increased as the groove width was increased (right column). DRG: Dorsal root ganglion; PLGA: poly(lactic-co-glycolic acid); DAPI: 4',6-diamidino-2-phenylindole.

on the 10 $\mu\text{m}/10 \mu\text{m}$, 30 $\mu\text{m}/30 \mu\text{m}$, 100 $\mu\text{m}/30 \mu\text{m}$ micropatterned PLGA films, these combinations were used to investigate the neurite extension enhancing capabilities of the films when DRG neurons were grown on the films. The DRG's neurite extension and alignment behavior when grown on 10 $\mu\text{m}/10 \mu\text{m}$, 30 $\mu\text{m}/30 \mu\text{m}$, 100 $\mu\text{m}/30 \mu\text{m}$ micropatterned and flat PLGA films can be seen in Figure 5. Flat PLGA films were used as a control group. DRG neurons grown on the 10 $\mu\text{m}/10 \mu\text{m}$, 30 $\mu\text{m}/30 \mu\text{m}$ groups demonstrated the greatest neurite extension growing distances of 5.76 and 7.27 mm, respectively. The DRG neurons grown on the 100 $\mu\text{m}/30 \mu\text{m}$ films presented good alignment, but

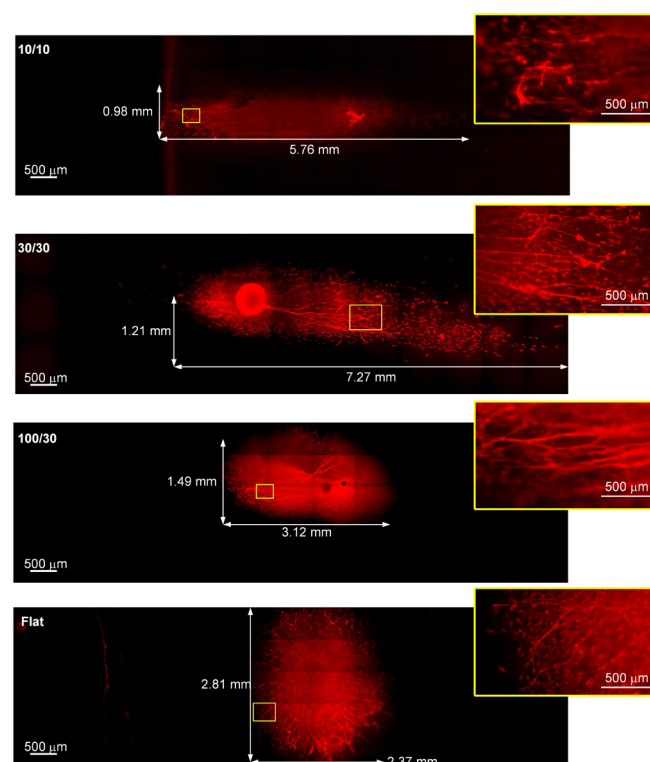


Figure 5 Immunolabeled DRG neurons grown on 10 $\mu\text{m}/10 \mu\text{m}$, 30 $\mu\text{m}/30 \mu\text{m}$, and 100 $\mu\text{m}/30 \mu\text{m}$ micropatterned and flat PLGA films. Whole DRGs were cultured on the micropatterned films to assess neurite extension. The red fluorescence labels beta-tubulin protein which is a neuronal marker. The magnified image is to show the alignment properties the ridges/groove combinations have on the neurites. 10 $\mu\text{m}/10 \mu\text{m}$, 30 $\mu\text{m}/30 \mu\text{m}$ micropatterned films showed the greatest neurite extension, 5.76 mm and 7.27 mm, respectively. DRGs grown on 100 $\mu\text{m}/30 \mu\text{m}$ micropatterned films and flat films grew with a shorter and uniform neurite distribution around the DRG, instead of extending outward along the patterns. Scale bars: 500 μm . DRG: Dorsal root ganglion; PLGA: poly(lactic-co-glycolic acid).

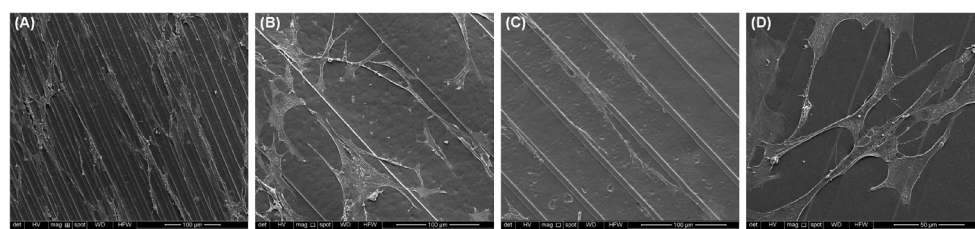


Figure 4 Scanning electron microscope images of dorsal root ganglion cells growing on 10 $\mu\text{m}/10 \mu\text{m}$ (A), 100 $\mu\text{m}/100 \mu\text{m}$ (B), 10 $\mu\text{m}/50 \mu\text{m}$ (C) and 50 $\mu\text{m}/10 \mu\text{m}$ (D) micropatterned poly(lactic-co-glycolic acid) films.

Visual representation of the better dorsal root ganglion cell alignment on the films with smaller ridges (A and C) compared to the films with larger ridges (B and D). Scale bars: 100 μm in A-C, 50 μm in D.

lower neurite extension (3.12 mm) in comparison to the 10 μm /10 μm and 30 μm /30 μm groups. When grown on flat films, the DRG cell growth and neurite extension were shorter, random, and non-oriented.

Discussion

Research has demonstrated techniques that produce micropatterns on materials, such as e-beam lithography, and femtosecond laser (Lu and Chen, 2004; Gomez et al., 2007; Lim et al., 2011). However, these fabrication techniques are high in cost when compared to photolithography. Additionally, these techniques usually require high-power to create the micropatterns, which could generate abundant particles and melting on the material surface. Hence, photolithography and micro-molding techniques were chosen to create micropatterned, bioresorbable PLGA films to construct peripheral nerve regeneration devices.

PLGA has been shown to hydrate and swell when exposed to water (Siegel, 2011). When exposed to water-rich cell culture medium, the micropatterned PLGA films experienced hydration and swelling. This was also observed in our study when the thickness increased after 7 days. Bulk degradation of PLGA films has been demonstrated by various previous studies. These studies explained that the degradation is faster in the center of the film compared to that on the surface due to a phenomenon called autocatalysis because of the increased concentration of acidic degradation products that accumulate inside the film. The heterogeneous surface degradation resulted in change in the surface of micropatterned PLGA films (Vey, 2012; Shirazi et al., 2014). Our findings were consistent with these previous studies. Degeneration primarily occurred inside the PLGA films, since the microholes observed were in the inner film rather than on the surface.

There is evidence that microstructure dimensions can be controlled to influence nerve cell alignment and migration on scaffolds (Qu et al., 2013). Previous studies have indicated that the width of microchannels has a significant influence on cell growth geometry and that different cell types have different responses to the width of microchannels. Schwann cells showed more parallel growth on 10 μm microchannels than on 20 μm micropatterns (Hsu et al., 2005). The neurites of PC12 cells showed more significant parallel growth on smaller micropatterns than on larger micropatterns (Hsu et al., 2005). Our study was consistent with these studies. The DRG neurons showed more significant parallel alignment and less branching on the 10 μm /10 μm patterns. Yao et al. (2009) presented that parallel neurite growth from PC12 cells occurred on micropatterned PLGA films, with more significant alignment found on micropatterned PLGA films with smaller groove widths of 5 μm . This suggested that smaller patterns provided better efficiency on cell guidance, because the tight ridges & grooves guide neurite extension by restricting the growth unidirectionally (Li et al., 2014). However, the cell alignment property is also controlled by the ratio of ridge/groove combination. When the ratio equals 1 (even group), the alignment efficiency depends on the size of pattern, the smaller (10 μm /10 μm

and 30 μm /30 μm) had better alignment and neurite extension, indicating that smaller cellular sized ridge/grooves are efficient at directing cell growth. If the ratio is smaller than 1 (larger grooves than ridges), the alignment efficiency increases as the width of the ridge decreases, since the nerve cells are sensitive on the edges of the pattern. Goldner et al. (2006) demonstrated that neurites will bridge across micropatterned grooves to help nerve cells to gain contact with the ridges. Therefore, the DRG neurons in this study easily crossed the smaller grooves to connect to both side ridges of a groove. When the ratio is larger than 1 (ridges are larger than grooves), the alignment efficiency reduces as the width of the groove decreases. This suggests that the overall lower groove area in these ridge control groups deters the DRG neurons for readily attaching and orienting to the micropattern surface. Our results indicate that DRG neurons prefer to interact and orient themselves around the corners and edges of ridges and grooves, and that higher densities of ridges and grooves on the 10 μm /10 μm and 30 μm /30 μm films provide a superior alignment capability. Additionally, the micropatterned PLGA films with the smaller width 10 μm /10 μm and 30 μm /30 μm combinations were the most effective at enhancing neurite extension. Cell alignment and neurite extension have critical implications in treating peripheral nerve gap injuries. Current clinically available nerve conduits lack the ability to promote neurite extension and cell proliferation across the empty volume in a gap injury, and they only provide gross directional guidance. The addition of micropatterned scaffolding into the inner lumen of a nerve conduit can promote and expedite neuronal cell ingrowth to more effectively cross the gap.

Su et al. (2013) demonstrated that grooved patterns can restrict the motility of PC12 cells and decrease the velocity of cellular movements on silicon wafers. Liu et al. (2016) presented that Schwann cell populations migrated the fastest on the smallest sized microgroove channels. The efficacy of cell migration on micropatterned substrates is dependent on the cell type. Joo used laminin (LN) and poly-L-lysine to define various micropatterns on the cell culture substrates to investigate the migration and differentiation of adult neural stem cells. Their data suggested that adult neural stem cells cultured on smaller groove patterned substrate showed higher potential for differentiation into neuron cells than larger groove patterned. Adult neural stem cells derived neurons presented lower migration abilities than astrocytes on 30 μm /30 μm patterned substrate (Joo et al., 2015). These studies suggest that alteration of the ridge spacing has the ability to restrict cell migration in one direction and increase neurite extension distances. But, to fully understand the mechanisms of cell migration on micropatterned substrates, further investigation is warranted. To summarize the implications of our results, a good micropattern ridge/groove combination for improving cell migration, alignment, and neurite extension must have properly chosen ridge and groove width parameters to fully optimize cell interactions. Width of the ridge and grooves must be similar to the size of a cell to provide optimal neural cell alignment and neurite alignment.

Conclusion

The micropatterned PLGA films with surface ridge/groove topography were successfully fabricated by combining photolithography and micro-modeling techniques. Material degradation testing showed degradation rate was about 2% (1 µg) per week and 0.28% (0.14 µg) per day. The PLGA films with the 10 µm/10 µm and 30 µm/30 µm combinations possessed the most effective DRG cell guidance and neurite extension. We demonstrated that cell alignment properties were dependent on the ratio of the ridge/groove parameters. When the ratio equaled 1 (even group), the DRG cell alignment and extension properties diminished as the ridge and groove width values increased. When the ratio was smaller than 1 (groove controlled group), the cell alignment efficacy increased as the ridge widths decreased. When the ratio was larger than 1 (ridge controlled group), the cell alignment efficacy decreased as the groove widths decreased. For DRG cell migration and extension studies, we demonstrated that the 10 µm/10 µm PLGA films showed good migration and extension, but 30 µm/30 µm PLGA film provided better migration and extension. The studied micropatterned PLGA films may offer a potential design for peripheral nerve regeneration devices. The micropatterned PLGA films can be used to line the inner walls of a nerve conduit to improve gap-repair functional recovery outcomes. This technology can also be extended to other biodegradable polymers for other tissue engineering applications.

Author contributions: CWL, JS, HS, BKG, and JA participated in conception and design of this study, definition of intellectual contents. CWL performed experiments and collected the data. CWL and BD analyzed the data and contributed to paper preparation. BD and JA edited the paper. BKG and JA reviewed the paper. JA was also the guarantor of this study. All authors approved the final version of this paper.

Conflicts of interest: There are no conflicts of interest to declare.

Financial support: None.

Research ethics: IACUC approval was not required for the experiments performed in this study in accordance with the University of Utah's IACUC Guidelines.

Data sharing statement: Datasets analyzed during the current study are available from the corresponding author on reasonable request.

Plagiarism check: Checked twice by iThenticate.

Peer review: Externally peer reviewed.

Open access statement: This is an open access article distributed under the terms of the Creative Commons Attribution-NonCommercial-ShareAlike 3.0 License, which allows others to remix, tweak, and build upon the work non-commercially, as long as the author is credited and the new creations are licensed under identical terms.

Open peer reviewers: Juanita Anders, Uniformed Services University of the Health Sciences, USA; A.A. Poot, University of Twente, Netherlands.

Additional file: Open peer review reports 1 and 2.

References

- Arslantunali D, Dursun T, Yucel D, Hasirci N, Hasirci V (2014) Peripheral nerve conduits: technology update. *Med Devices (Auckl)* 7:405-424.
- Battiston B, Geuna S, Ferrero M, Tos P (2005) Nerve repair by means of tubulization: literature review and personal clinical experience comparing biological and synthetic conduits for sensory nerve repair. *Microsurgery* 25:258-267.
- Bini TB, Gao S, Tan TC, Wang S, Lim A, Hai LB, Ramakrishna S (2004) Electrospun poly(L-lactide-co-glycolide) biodegradable polymer nanofibre tubes for peripheral nerve regeneration. *Nanotechnology* 15:1459-1464.
- Daly WT, Knight AM, Wang H, de Boer R, Giusti G, Dadsetan M, Spinner RJ, Yaszemski MJ, Windebank AJ (2013) Comparison and characterization of multiple biomaterial conduits for peripheral nerve repair. *Biomaterials* 34:8630-8639.
- Goldner JS, Bruder JM, Li G, Gazzola D, Hoffman-Kim D (2006) Neurite bridging across micropatterned grooves. *Biomaterials* 27:460-472.
- Gomez N, Lee JY, Nickels JD, Schmidt CE (2007) Micropatterned polypyrrole: a combination of electrical and topographical characteristics for the stimulation of cells. *Adv Funct Mater* 17:1645-1653.
- Hsu SH, Chen CY, Lu PS, Lai CS, Chen CJ (2005) Oriented Schwann cell growth on microgrooved surfaces. *Biotechnol Bioeng* 92:579-588.
- Joo S, Kim JY, Lee E, Hong N, Sun W, Nam Y (2015) Effects of ECM protein micropatterns on the migration and differentiation of adult neural stem cells. *Sci Rep* 5:13043.
- Labroo P, Shea J, Sant H, Gale B, Agarwal J (2017) Effect Of combining FK506 and neurotrophins on neurite branching and elongation. *Muscle Nerve* 55:570-581.
- Li G, Zhao X, Zhao W, Zhang L, Wang C, Jiang M, Gu X, Yang Y (2014) Porous chitosan scaffolds with surface micropatterning and inner porosity and their effects on Schwann cells. *Biomaterials* 35:8503-8513.
- Lim YC, Johnson J, Fei Z, Wu Y, Farson DF, Lannutti JJ, Choi HW, Lee LJ (2011) Micropatterning and characterization of electrospun poly(epsilon-caprolactone)/gelatin nanofiber tissue scaffolds by femtosecond laser ablation for tissue engineering applications. *Biotechnol Bioeng* 108:116-126.
- Liu C, Kray J, Toomajian V, Chan C (2016) Schwann cells migration on patterned polydimethylsiloxane microgrooved surface. *Tissue Eng Part C Methods* 22:644-651.
- Lu Y, Chen SC (2004) Micro and nano-fabrication of biodegradable polymers for drug delivery. *Adv Drug Deliv Rev* 56:1621-1633.
- Mobasser SA, Terenghi G, Downes S (2013) Micro-structural geometry of thin films intended for the inner lumen of nerve conduits affects nerve repair. *J Mater Sci Mater Med* 24:1639-1647.
- Navarro X, Vivo M, Valero-Cabre A (2007) Neural plasticity after peripheral nerve injury and regeneration. *Prog Neurobiol* 82:163-201.
- Qu J, Wang D, Wang H, Dong Y, Zhang F, Zuo B, Zhang H (2013) Electrospun silk fibroin nanofibers in different diameters support neurite outgrowth and promote astrocyte migration. *J Biomed Mater Res A* 101:2667-2678.
- Reichenberger MA, Mueller W, Hartmann J, Diehm Y, Lass U, Koellensperger E, Leimer U, Germann G, Fischer S (2016) ADSCs in a fibrin matrix enhance nerve regeneration after epineurial suturing in a rat model. *Microsurgery* 36:491-500.
- Shirazi RN, Aldabbagh F, Erxleben A, Rochev Y, McHugh P (2014) Nanomechanical properties of poly(lactic-co-glycolic) acid film during degradation. *Acta Biomater* 10:4695-4703.
- Siegel HK, MaSJ (2011) Poly lactic-co-glycolic acid (PLGA) as biodegradable controlled drug delivery carrier. *Polymers* 3:1377-1397.
- Su WT, Liao YF, Wu TW, Wang BJ, Shih YY (2013) Microgrooved patterns enhanced PC12 cell growth, orientation, neurite elongation, and neurogenesis. *J Biomed Mater Res A* 101:185-194.
- Sudwilai T, Ng JJ, Boonkrai C, Israsena N, Chuangchote S, Supaphol P (2014) Polypyrrole-coated electrospun poly(lactic acid) fibrous scaffold: effects of coating on electrical conductivity and neural cell growth. *J Biomater Sci Polym Ed* 25:1240-1252.
- Veya E, Rodger C, Meehan L, Booth J, Claybourn M, Miller AF, Saiani A (2012) The impact of chemical composition on the degradation kinetics of poly(lactic-co-glycolic) acid copolymers cast films in phosphate buffer solution. *Polym Degr Stab* 97:358-365.
- Yang F, Murugan R, Wang S, Ramakrishna S (2005) Electrospinning of nano/micro scale poly(L-lactic acid) aligned fibers and their potential in neural tissue engineering. *Biomaterials* 26:2603-2610.
- Yao L, Wang S, Cui W, Sherlock R, O'Connell C, Damodaran G, Gorman A, Windebank A, Pandit A (2009) Effect of functionalized micropatterned PLGA on guided neurite growth. *Acta Biomater* 5:580-588.

(Copyedited by Li CH, Song LP, Zhao M)